Discovering ditauonium(n^3S_1) in $e^+e^- \to \mu^+\mu^-$ process

Jing-Hang Fu

Coauthor: Yu-Jie Zhang

fujinghang@buaa.edu.cn
Beihang University

Aug. 22-24, 2022, Hangzhou

Outline

1. **Introduction**
   - Leptonium
   - Ditauonium spectroscopy
2. **Calculation frame**
   - Feynman diagram and Feynman amplitude
   - Cross section
   - Smearing effect
3. **Result**
   - Input parameters
   - Result without smearing effect
   - Result within smearing effect
4. **Summary**

Introduction

Leptonium

- Lepton and Antilepton($e^{\pm}, \mu^{\pm}, \tau^{\pm}$) can form transient bound states under QED interaction.
- 6 possible exotic leptonic atoms ($e^{+}e^{-}$), ($e^{\pm}\mu^{\mp}$), ($\mu^{+}\mu^{-}$), ($e^{\pm}\tau^{\mp}$), ($\mu^{\pm}\tau^{\mp}$), ($\tau^{+}\tau^{-}$).
- Only two bound states(($e^{+}e^{-}$) in 1951, ($e^{\pm}\mu^{\mp}$) in 1960) have been observed.

- The ditauonium Bohr radius $a_0 = 30.4\ \mathrm{fm}$(1/1743 of Bohr radius of hydrogen atom) is the smallest of all leptonium systems.
- Also ditauonium is the most strongly bound of all leptonia only by QED interaction.

Ditauonium

S wave(L=0)

Para-ditauonium($^1S_0$), S=0, $\eta_\tau(J^{PC}=0^{-+})$
Ortho-ditauonium($^3S_1$), S=1, $J_\tau(J^{PC}=1^{--})$

P wave(L=1)

S=0, $h_\tau(J^{PC}=1^{+-})$
S=1, $\chi_{\tau 0}(J^{PC}=0^{++}), \chi_{\tau 1}(J^{PC}=1^{++}), \chi_{\tau 2}(J^{PC}=2^{++})$

Ditauonium spectroscopy

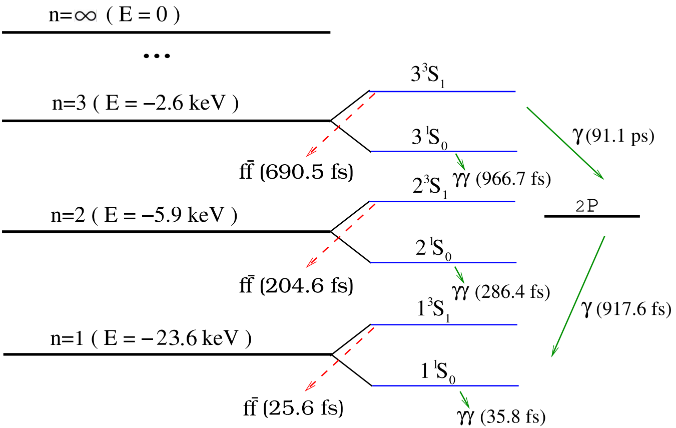

Figure: Ditauonium spectroscopy, from 2204.07269

Energy levels

At Leading-order, the energy levels can be described by the Schrödinger equation with the Coulomb potential.

$$E_{\mathrm{n}} = -\frac{\alpha^2 m_\tau}{4n^2} \approx -\frac{23.655\ \mathrm{keV}}{n^2}$$

And at LO, the square of the *nS* wavefunction at the radial origin($r = 0$),

$$|\varphi_{n\mathrm{S}}(r = 0)|^2 = \frac{(\alpha m_\tau)^3}{8\pi n^3}$$

Ditauonium mass

Ditauonium mass is

$$
\begin{aligned}
m_{n^3S_1} &= 2m_\tau + E_n \\
m_\tau &= 1776.86 \pm 0.12\ \mathrm{MeV} \\
2m_\tau &\approx 3553.72 \pm 0.24\ \mathrm{MeV}
\end{aligned}
$$

$$
\begin{aligned}
m_{1^3S_1} &\approx 3353.696 \pm 0.24\ \mathrm{MeV} \\
m_{2^3S_1} &\approx 3353.714 \pm 0.24\ \mathrm{MeV} \\
m_{3^3S_1} &\approx 3353.717 \pm 0.24\ \mathrm{MeV}
\end{aligned}
$$

Decay widths

At Leading-order, ditauonium(n^3S_1) decays into pairs of fermions lighter than half the ditauonium mass, through an intermediate sigle photon. ($f = e, \mu, u, d, s$)

$$\Gamma^{(0)}(n^3S_1 \to f\bar{f}) = N_{c,f} Q_f^2 \frac{\alpha^5 m_\tau}{6\, n^3} \left(1 + \frac{m_f^2}{m_{n^3S_1}^2}\right) \sqrt{1 - \frac{m_f^2}{m_\tau^2}}$$

The zeroth-order dilepton decay

$$\Gamma^0(n^3S_1 \to e^+e^-, \mu^+\mu^-) = \frac{\alpha^5 m_\tau}{6n^3}$$

The zeroth-order quark-pair decay

$$\Gamma^0(n^3S_1 \to q\bar{q}) \approx 2.2 \frac{\alpha^5 m_\tau}{6n^3}$$

Decay widths

$$\Gamma(n^3S_1 \to f\bar{f}) \approx 4.2\frac{\alpha^5 m_\tau}{6n^3}$$

Any of the two tau leptons decays through the weak interaction,

$$2\Gamma(\tau \to X) = \frac{2}{290.3\ \mathrm{fs}} = 4.5346 \pm 0.008\ \mathrm{meV}$$

For n=3, also add

$$\begin{aligned}\Gamma^0(3S \to 2P) &= \left(\frac{2}{5}\right)^9 \frac{3\alpha^5 m_\tau}{4} \approx 0.00724\ \mathrm{meV}\\ \Gamma^0(2P \to 1S) &= \left(\frac{2}{3}\right)^8 \frac{\alpha^5 m_\tau}{2} \approx 0.718\ \mathrm{meV}\end{aligned}$$

Decay widths

In summary,

$$
\begin{aligned}
\Gamma_{total}(1^3S_1) &= \Gamma(1^3S_1 \to f\bar{f}) + 2\Gamma(\tau \to X) \\
&\approx 30.924 \text{ meV} \\
\Gamma_{total}(2^3S_1) &= \Gamma(2^3S_1 \to f\bar{f}) + 2\Gamma(\tau \to X) \\
&\approx 7.833 \text{ meV} \\
\Gamma_{total}(3^3S_1) &= \Gamma(3^3S_1 \to f\bar{f}) + 2\Gamma(\tau \to X) + \Gamma^0(3S \to 2P) \\
&\approx 5.519 \text{ meV}
\end{aligned}
$$

Decay widths

The annihilation decay widths($\mathcal{O}(\alpha^7)$) of P-wave are comparatively negligible.

$$\frac{\Gamma(2P \to 1S)}{\Gamma_{total}(2P)} = \frac{\Gamma(2P \to 1S)}{\Gamma(2P \to 1S) + 2\Gamma(\tau \to X)} \approx 13.67\%$$

Thus

$$\Gamma(3^3S_1 \to l^+l^-\gamma\gamma) = \Gamma^0(3S \to 2P) \cdot \frac{\Gamma(2P \to 1S)}{\Gamma_{total}(2P)} \cdot \frac{\Gamma(1^3S_1 \to l^+l^-)}{\Gamma_{total}(1^3S_1)}$$

$$\Gamma(3^3S_1 \to l^+l^-(\gamma\gamma)) = \Gamma(3^3S_1 \to l^+l^-) + \Gamma(3^3S_1 \to l^+l^-\gamma\gamma)$$

Decay widths

Table: $\Gamma(n^3S_1 \to e^+e^-/\mu^+\mu^-)$

	$1^3S_1 \to l^+l^-$	$2^3S_1 \to l^+l^-$	$3^3S_1 \to l^+l^-(\gamma\gamma)$
$\Gamma(l^+l^-)$	6.136 meV	0.767 meV	0.227 meV
Γ_{total}	30.924 meV	7.833 meV	5.519 meV
B_r	19.8%	9.8%	4.1%

Calculation frame

Feynman diagram

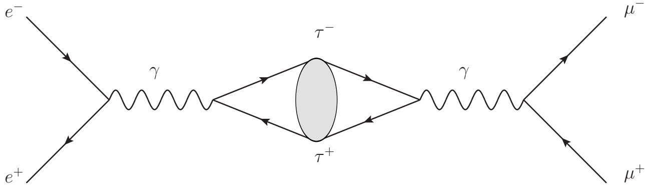

Figure: Feynman diagram of $e^+e^- \to \tau^+\tau^-(n^3S_1) \to \mu^+\mu^-$.

Feynman amplitude of signal is

$$A(e^-e^+ \to n^3S_1 \to \mu^-\mu^+)$$
$$= A(e^-e^+ \to n^3S_1)\frac{i}{s - m^2_{n^3S_1} + im_{n^3S_1}\Gamma}A(n^3S_1 \to \mu^-\mu^+)$$

Feynman amplitude of signal

For S wave, nonrelativistic perturbation,

$$
\begin{aligned}
&A(e^- e^+ \to n^3 S_1) \\
&= \sum_{s_{3z}, s_{4z}, S_z, L_z} \langle s_3, s_{3z}; s_4, s_{4z} | S, S_z \rangle \langle S, S_z; L, L_z | J, J_z \rangle \\
&\times \int \frac{dq^3}{(2\pi)^{3/2}} A(e^-(p_1) e^+(p_2) \to \tau^-(q/2, s_3) \tau^+(q/2, s_4)) \phi(0)
\end{aligned}
$$

$A(n^3 S_1 \to \mu^- \mu^+)$ is similar.

Signal-background interference

Square of amplitude

$$
\begin{aligned}
&|A(e^-e^+ \to \mu^-\mu^+) + A(e^-e^+ \to \tau^-\tau^+(n^3S_1) \to \mu^-\mu^+)|^2 \\
&= |A(e^-e^+ \to \mu^-\mu^+)|^2 \\
&+|A(e^-e^+ \to \tau^-\tau^+(n^3S_1) \to \mu^-\mu^+)|^2 \\
&+A(e^-e^+ \to \mu^-\mu^+) \times A(e^-e^+ \to \tau^-\tau^+(n^3S_1) \to \mu^-\mu^+)^* \\
&+A(e^-e^+ \to \mu^-\mu^+)^* \times A(e^-e^+ \to \tau^-\tau^+(n^3S_1) \to \mu^-\mu^+)
\end{aligned}
$$

$$
\frac{d\sigma}{d\Omega} = \frac{1}{64\pi^2 E_{cm}^2}|\bar{A}|^2
$$

Breit-Wigner formula, from PDG2020

Resonant cross sections are generally described by the Breit-Wigner formula,

$$\sigma(E) = \frac{2J+1}{(2S_1+1)(2S_2+1)} \frac{4\pi}{k^2} \left[\frac{\Gamma^2/4}{(E-E_0)^2+\Gamma^2/4} \right] B_{in} B_{out}$$

The branching fraction for the resonance into the initial-state channel is B_{in} and into the final-state channel is B_{out}. For a narrow resonance,

$$\sigma(E) = \frac{2J+1}{(2S_1+1)(2S_2+1)} \frac{4\pi}{k^2} \frac{\pi\Gamma\delta(E-E_0)}{2} B_{in} B_{out}$$

Breit-Wigner formula

For n^3S_1,

$$J = 1, S_1 = S_2 = \frac{1}{2}, k^2 \approx m_\tau^2$$

Breit-wigner formula become

$$\sigma(E) = \frac{3\pi}{m_\tau^2}\left[\frac{\Gamma^2/4}{(E-E_0)^2+\Gamma^2/4}\right] B_{in}B_{out}$$

$$\sigma(E) = \frac{3\pi}{m_\tau^2}\frac{\pi\Gamma\delta(E-E_0)}{2} B_{in}B_{out}$$

Smearing effect, from 1505.03930

The finite experimental resolution will smear the peak.
Smearing effect:

$$\sigma_{ex}(E) = \int \sigma_{th}(E_{cm}) \frac{1}{\sigma_{MR}\sqrt{2\pi}} \exp\left[-\frac{(E-E_{cm})^2}{2\sigma_{MR}^2}\right] dE_{cm}.$$

Breit-wigner formula

$$\sigma_{th}(E_{cm}) = \frac{3\pi}{m_\tau^2} \frac{\pi\Gamma\delta(E_{cm}-E_0)}{2} B_{in}B_{out},$$

$$\sigma_{ex}(E) = \frac{3\pi}{m_\tau^2} \frac{\pi\Gamma}{2} B_{in}B_{out} \frac{1}{\sigma_{MR}\sqrt{2\pi}} \exp\left[-\frac{(E-E_0)^2}{2\sigma_{MR}^2}\right]$$

Smearing effect

Then the peak value is($E = E_0$)

$$\sigma_{ex}(E_0) = \frac{3\pi^2\Gamma}{2m_\tau^2} B_{in} B_{out} \frac{1}{\sigma_{MR}\sqrt{2\pi}}$$

Result

Input parameters, from PDG2020

Fermion mass

$m_e = 0.5109989461 \pm 0.0000000031\ \mathrm{MeV}$
$m_\mu = 105.6583745 \pm 0.0000024\ \mathrm{MeV}$
$m_\tau = 1776.86 \pm 0.12\ \mathrm{MeV}$

Parameters

$\alpha = 1/137$
$2\Gamma_\tau = 4.5346 \pm 0.008\ \mathrm{meV}$
$m_{1^3S_1} = 3353.696 \pm 0.24\ \mathrm{MeV}$
$m_{2^3S_1} = 3353.714 \pm 0.24\ \mathrm{MeV}$
$m_{3^3S_1} = 3353.717 \pm 0.24\ \mathrm{MeV}$

Result of 1^3S_1 without smearing effect

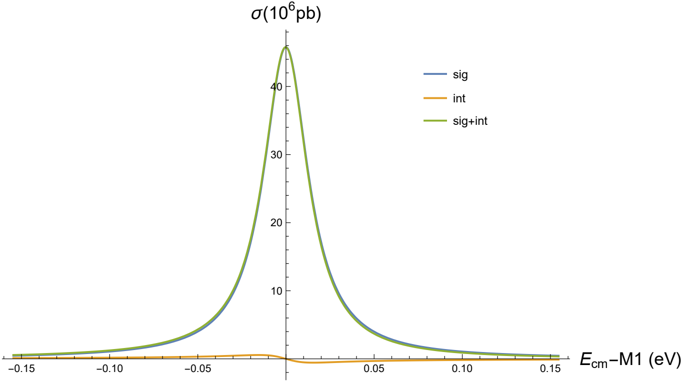

Figure: The invariant mass distribution of signal and interference without smearing effect. The peak value of signal is 45.768 μb, and the peak value of interference is 0.561 μb.

Result of 2^3S_1 without smearing effect

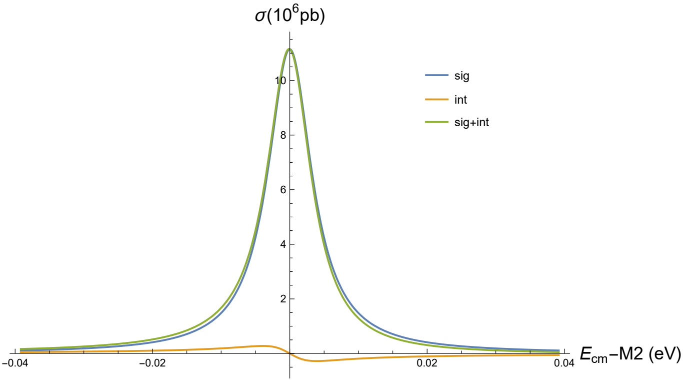

Figure: The invariant mass distribution of signal and interference without smearing effect. The peak value of signal is 11.145 μb, and the peak value of interference is 0.277 μb.

Result of 3^3S_1 without smearing effect

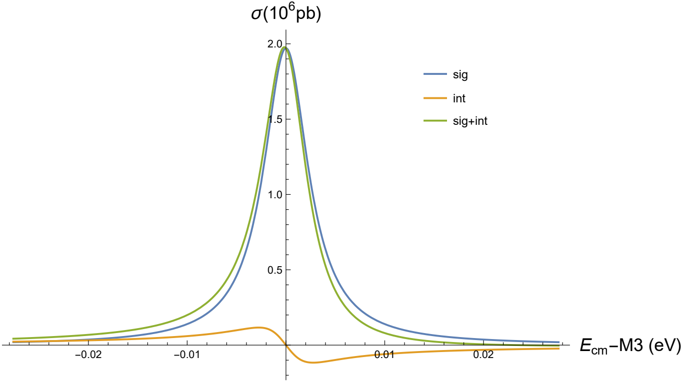

Figure: The invariant mass distribution of signal and interference without smearing effect. The peak value of signal is 1.974 μb, and the peak value of interference is 0.116 μb.

Result of 1^3S_1 within smearing effect

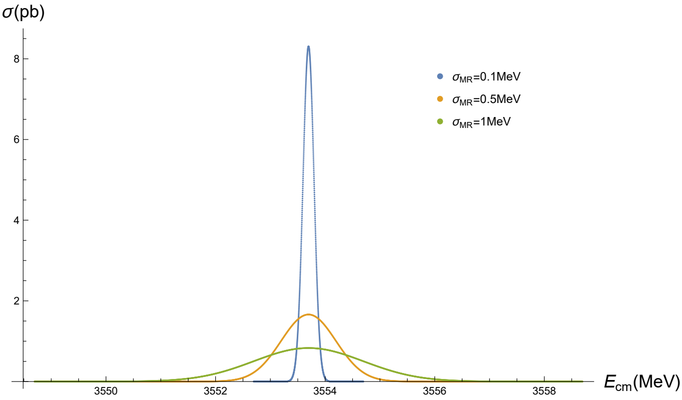

Figure: The invariant mass distribution of signal and interference within smearing effect. The peak values are 8.869 pb, 1.774 pb, 0.887 pb.

Result of 2^3S_1 within smearing effect

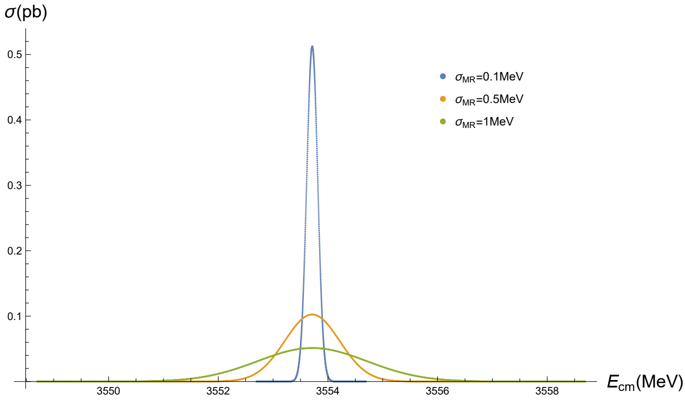

Figure: The invariant mass distribution of signal and interference within smearing effect. The peak values are 0.547 pb, 0.109 pb, 0.055 pb.

Result of 3^3S_1 within smearing effect

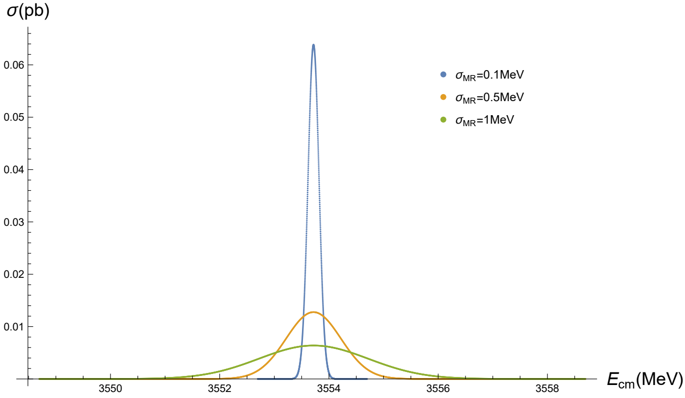

Figure: The invariant mass distribution of signal and interference within smearing effect. The peak values are 0.068 pb; 0.014 pb; 0.007 pb.

Result of all within smearing effect

Table: Cross section(Breit-wigner) within smearing effect(σ_{MR}=0.1 MeV, 0.5 MeV, 1 MeV).

States	Cross section		
σ_{MR}	0.1 MeV	0.5 MeV	1 MeV
$e^+e^- \to \mu^+\mu^-$	6881.45 pb		
$1^3S_1 \to \mu^+\mu^-$	8.869 pb	1.774 pb	0.887 pb
$2^3S_1 \to \mu^+\mu^-$	0.547 pb	0.109 pb	0.055 pb
$3^3S_1 \to \mu^+\mu^-$	0.068 pb	0.014 pb	0.007 pb
all of signal	9.485 pb	1.897 pb	0.948 pb

Result of all within smearing effect

Table: Cross section(Breit-wigner) within smearing effect(σ_{MR}=0.1 MeV, 0.5 MeV, 1 MeV).

States	Cross section		
σ_{MR}	0.1 MeV	0.5 MeV	1 MeV
$e^+e^- \to \mu^+\mu^-/LH$	22020.6 pb		
$1^3S_1 \to \mu^+\mu^-/LH$	28.381 pb	5.676 pb	2.838 pb
$2^3S_1 \to \mu^+\mu^-/LH$	1.751 pb	0.350 pb	0.175 pb
$3^3S_1 \to \mu^+\mu^-/LH$	0.219 pb	0.0437 pb	0.022 pb
all of signal	30.351 pb	6.070 pb	3.035 pb

Result of all within smearing effect($\mu^+\mu^-/LH, \sigma_{MR} = 1\ \mathrm{MeV}$)

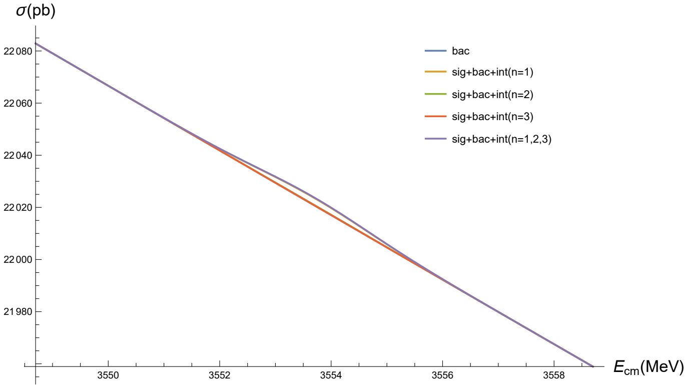

Figure: The invariant mass distribution of signal, interference and background within smearing effect($\sigma_{MR} = 1\ \mathrm{MeV}$).

Result of all within smearing effect($\mu^+\mu^-/LH, \sigma_{MR} = 1$ MeV)

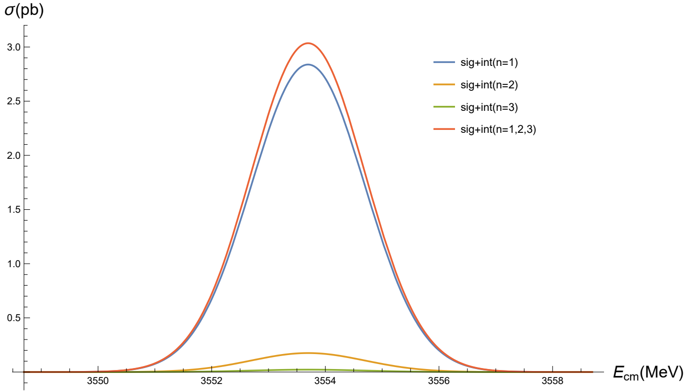

Figure: The invariant mass distribution of signal and interference within smearing effect($\sigma_{MR} = 1$ MeV).

Events estimated($\sigma_{MR} = 1$ MeV)

$$\text{Events} = \sigma \cdot \mathcal{L}$$

Table: Estimate events with integrated luminosity $\mathcal{L} = 100\ \mathrm{fb}^{-1}$ (BES III, σ_{MR}=1 MeV).

States	Events($\mu^+\mu^-$)	Significance	Events($\mu^+\mu^- + LH$)	Significance
Background	688142617		2202056374	
1^3S_1	88693	3.381 σ	283817	6.048 σ
2^3S_1	5471	0.209 σ	17507	0.373 σ
3^3S_1	683	0.026 σ	2185	0.047 σ
all of signal	94847	3.616 σ	303509	6.468 σ

Events estimated($\sigma_{MR} = 0.5$ MeV)

Table: Estimate events with integrated luminosity 100 fb^{-1} (σ_{MR}=0.5 MeV).

States	Events($\mu^+\mu^-$)	Significance	Events($\mu^+\mu^- + LH$)	Significance
Background	688142617		2202056374	
n=1	177385	6.762 σ	567634	12.096 σ
n=2	10942	0.417 σ	35014	0.746 σ
n=3	1366	0.052 σ	4370	0.093 σ
all of signal	189693	7.231 σ	607018	12.936 σ

$^1S_0 \to \gamma\gamma$

$^1S_0 \to \gamma\gamma$, from 2202.02316.

Colliding system, c.m. energy, $\mathcal{L}_{\rm int}$, exp.	$\sigma \times \mathcal{B}_{\gamma\gamma}$						$N \times \mathcal{B}_{\gamma\gamma}$	
	$\eta_c(1S)$	$\eta_c(2S)$	$\chi_{c,0}(1P)$	$\chi_{c,2}(1P)$	LbL	$\mathcal{T}_0$	$\mathcal{T}_0$	$\chi_{c,2}(1P)$
e^+e^- at 3.78 GeV, 20 fb^{-1}, BES III	120 fb	3.6 ab	15 ab	13 ab	30 ab	0.25 ab	–	–
e^+e^- at 10.6 GeV, 50 ab^{-1}, Belle II	1.7 fb	0.35 fb	0.52 fb	0.77 fb	1.7 fb	0.015 fb	750	38 500
e^+e^- at 91.2 GeV, 50 ab^{-1}, FCC-ee	11 fb	2.8 fb	3.9 fb	6.0 fb	12 fb	0.11 fb	5 600	$3 \cdot 10^5$
p-p at 14 TeV, 300 fb^{-1}, LHC	7.9 fb	2.0 fb	2.8 fb	4.3 fb	6.3 fb	0.08 fb	24	1290
p-Pb at 8.8 TeV, 0.6 pb^{-1}, LHC	25 pb	6.3 pb	8.7 pb	13 pb	21 pb	0.25 pb	0.15	8
Pb-Pb at 5.5 TeV, 2 nb^{-1}, LHC	61 nb	15 nb	21 nb	31 nb	62 nb	0.59 nb	1.2	62

$^1S_0 \to \gamma\gamma$

$^1S_0 \to \gamma\gamma$, from 2202.02316.

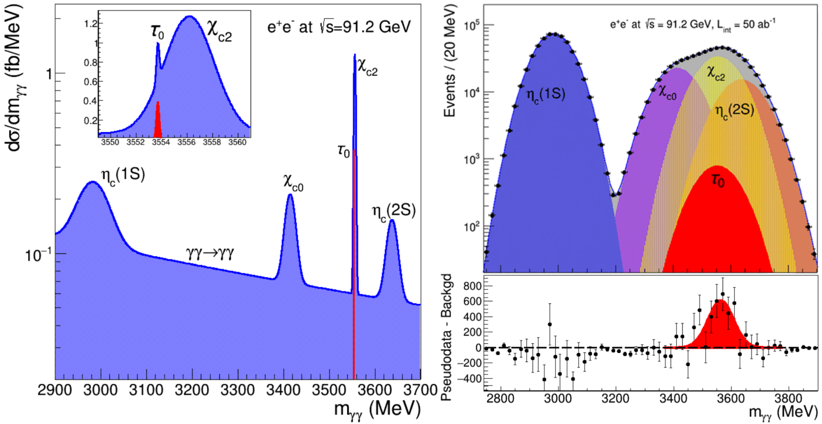

Summary

Summary

Summary

- We have presented the first feasibility study to produce and observe the bound state of two tau leptons, the heaviest and most compact purely leptonic "atomic" system.
- Ditauonium remains experimentally unobserved to date, and can be exploited for novel bound-state QED tests sensitive to physics beyond the standard model.
- Measurements of ditauonium can be used in high precision tests of QED and mass of tau lepton.
- ...